Power Cycling 101: Optimizing Energy Use in Advanced Sensor Products

By Mark Looney

Introduction

Highly integrated, fully specified sensor systems, such as the ADIS16209 tilt sensor (see Appendix), available in compact packages at attractive prices, allow system developers to readily use sensors that embrace technologies with which they may have little experience—with minimal investment and risk. Since accuracy is fully specified at a given power level, it might appear that the developer's ability to reduce power consumption is constrained. However, the use of power cycling provides an opening for reducing average power consumption in applications where energy use must be tightly managed. This article focuses on power cycling and its impact on overall power consumption.

Many of us grew up in homes with loving parents who would yell, "Turn off the lights when you leave the room! We don't own the power company!" In effect, they were teaching us an important energy management technique—*power cycling*—the process of removing power from a function when it is not needed, such as shutting off a sensor system when measurements are not required. This enables a reduction in average power dissipation, as quantified by the following equation:

$$P_{AVG} = [D \times P_{ON}] + [(1 - D) \times P_{OFF}]$$

$$D = \frac{T_{ON}}{T_{ON} + T_{OFF}} = duty\ cycle$$

$$P_{ON} = on \text{ power}, P_{OFF} = off \text{ power}$$

$$T_{ON} = on \text{ time}, T_{OFF} = off \text{ time}$$

P_{ON} is the system's power dissipation in its normal operating state. P_{OFF} is the system's overhead in its *off* state. Associated with residual currents, such as maintaining a power switch or a shutdown mode in a power regulator, it is typically on the order of 1 μA. The *on* time (T_{ON}) is the amount of time for the sensor system to turn on, produce a desired measurement, and turn back off. The *off* time (T_{OFF}) depends on how frequently the system requires sensor measurements. If the *off* power is much smaller than the *on* power, the average power dissipation is essentially proportional to the duty cycle. For example, if the *off* power is zero and the duty cycle is 10%, the average power dissipation is 10% of the normal operating power.

Sensor System Review

Transducers translate physical phenomena—such as temperature, acceleration, or strain—into electrical signals. To be used appropriately, transducer elements require support functions, such as excitation, signal conditioning, filtering, offset- and gain adjustment, and temperature compensation. Advanced sensor products also include analog-to-digital conversion and provide all these functions in a single package, delivering complete, calibrated sensor-to-bits functions. By eliminating the user's need to develop component-level designs or complex characterization and correction formulas, they enable faster design cycles with less investment. Although highly integrated sensor products reduce the burden of making circuit-level design decisions, it is helpful to understand their internal operation when considering power cycling to reduce average power.

Figure 1 shows many of the functions associated with a complete sensor system. Each transducer element requires an *interface circuit* to convert the physical change in the element into an electrical signal usable by standard signal processing components. For example, resistance strain gages—resistors that experience a change in resistance when subjected to a change in strain—are commonly used in the form of bridge circuits (with excitation) to convert the variable resistance into an electrical signal. Another example is *integrated micro-electromechanical systems* (*i*MEMS®) inertial sensors, such as accelerometers and gyroscopes. Their tiny structures respond to inertial motion changes with displacement changes between plates, which results in capacitance changes between electrical nodes. The interface circuit for the variable capacitive element typically uses a combination of modulation and demodulation stages to translate the capacitance change into an electrical signal.

The *buffer* stage, which prepares the signal for the input stage of the *analog-to-digital converter* (ADC), can include level shifting, gain, offset correction, buffering, and filtering. Once the sensor signal has been digitized, digital processing functions help increase the value of the information. *Digital filtering*, $h(n)$, reduces noise and focuses on the frequency band of interest. For example, a machine-health system might use a band-pass filter to focus on the frequency signature associated with a common wear-out mechanism. Other sensors, which need a stable dc reference, may place more value on a low-pass filter.

Sensor accuracies may differ substantially across a population of parts. In order to tighten the error distribution and increase the measurement certainty, sensor systems often include a *calibration* process that characterizes each sensor under known stimuli and conditions and provides unit-specific formulas that correct the output over all expected operating conditions. The final processing stage, $f(n)$, represents specific processing—for example, the trigonometric relationship used to translate an accelerometer's static gravitational measurements into orientation angles.

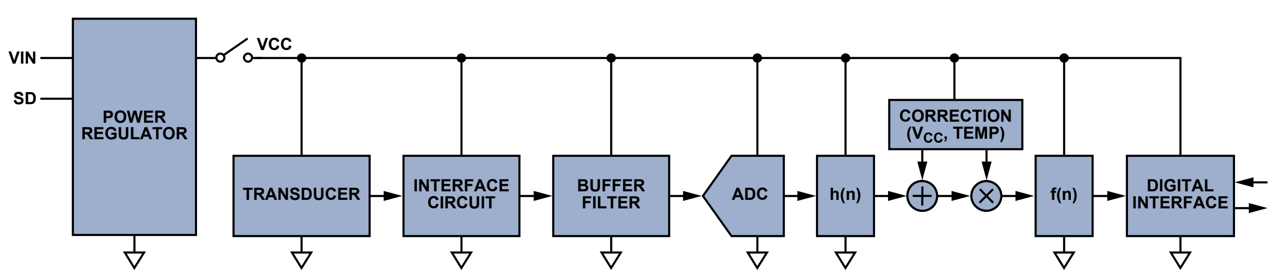

Figure 1. Example of a sensor system.

Power Cycling Considerations

When evaluating the effectiveness of power cycling in a sensor system, the designer must be sure to determine the time it takes to acquire useful data. Figure 2 shows how a typical sensor system responds when power is applied. T_M is the measurement time and T_C is the cycle time. The measurement time depends on the start-up time, T_1, the settling time, T_2, and the data-acquisition time, T_3.

The *start-up time* depends on the system processor and the initialization routines it must run to support sensor data sampling and signal-processing operations. When using a highly integrated sensor system, the start-up time is normally specified in the product documentation. Products of this type sometimes offer a *sleep* mode—which provides faster start-up times at the expense of higher power-off dissipation than *shutdown* mode.

Settling time can include electrical behavior of the transducer, interface circuit, filter, and physical components, as well as thermal and mechanical settling time. In some cases, these transient behaviors settle during the turn-on time, so they have little or no impact on the overall measurement time. The most conservative approach to analyzing the behaviors, however, is to consider that they happen in cascade, unless further analysis and research can support the more favorable assumption of simultaneous startup and settling.

The *data-acquisition time* depends on how many data samples are required, how fast the system processor can read data, and how soon the processor is available once accurate data is ready for acquisition.

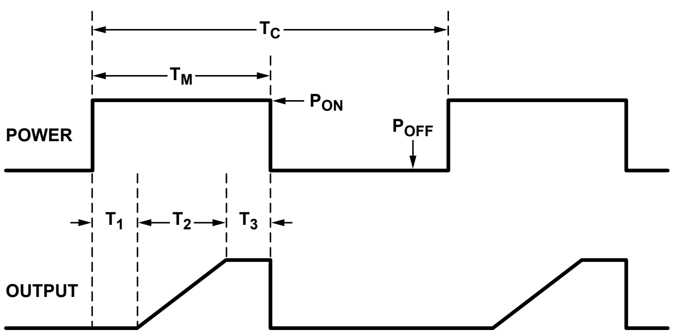

Figure 2. Sensor response during power cycling.

Analysis Example

This example evaluates a fully integrated MEMS tilt sensor to identify parameters that impact accuracy and measurement times in order to determine the important power vs. performance relationships. The following four steps provide a simple guideline for this process:

1. Learn how the sensor operates.
2. Capture relevant information from the product documentation.
3. Estimate important parameters that are not directly specified.
4. Develop power vs. performance relationships.

1. Operational Understanding

The example tilt sensor system is very similar to the generic system in Figure 1. The core MEMS accelerometer includes both the transducer element and the interface circuit. The accelerometer signal passes through a single-pole, low-pass filter, which limits the signal bandwidth to 50 Hz. The analog-to-digital converter runs at a sample rate of 200 SPS and feeds its output into the digital processing stage. The digital processing functions include an averaging filter, temperature-driver correction formulas, mathematical function for translating static accelerometer readings into inclination angles, user interface registers, and a serial interface.

When the accelerometer's measurement axis is perpendicular to gravity, its output will be zero, assuming zero bias error. It will produce an output of +1 *g* or –1 *g* when its measurement axis is parallel to gravity, with the polarity depending on its direction. The relationship between the static acceleration measurement and the inclination angle is a simple sine or tangent function, as shown in Figure 3. This analysis focuses on the *horizontal* mode (sine).

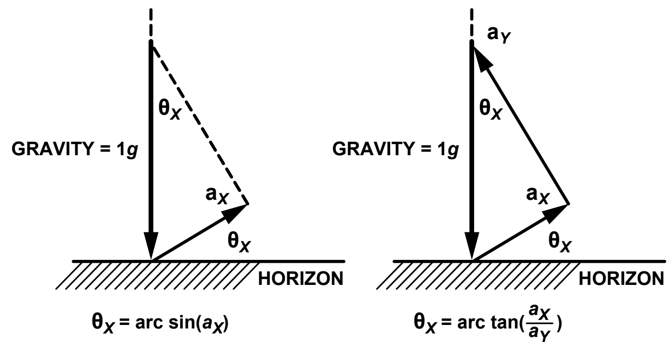

Figure 3. MEMS tilt sensor operation.

2. Capture Relevant Information from Product Literature

Table 1 provides an overview of the parameters that influence power cycling for an advanced sensor system. Some of these parameters are available in product data sheets, while others require analysis with respect to end-system performance goals. P_{ON} and T_1 are parameters from the data sheet. The remaining parameters can be used to estimate T_2 and T_3. The off-mode power comes from the shutdown current of the linear regulator.

Table 1. Sensor System Operating Specifications

Parameter	Value
Power supply	+3.3 V
Power, normal operation	46.2 mW (P_{ON})
Power, off-mode	3.3 μW (P_{OFF})
Power, sleep-mode	1.2 mW (P_{OFFS})
Turn-on time	190 ms (T_1)
Sleep-mode recovery	2.5 ms (T_{1S})
Accelerometer range	±1.7 *g*
Inclination angle range	±30°
Low-pass filter	–3 dB @ 50 Hz, single-pole
Sample rate	200 SPS
Digital filter	Running average, 256 max

3. Use Educated Assumptions to Quantify Remaining Influential Factors

The settling time influences the accuracy and measurement rate that a sensor system can support. Many different things can influence settling time, but this analysis focuses on the electrical factors. Estimating the settling time requires a performance objective, some key assumptions, and a model for analyzing the sensor's response to power application. The first key assumption is that the filter settling happens after the initial start-up period (turn-on time). While these two periods can be simultaneous, analyzing them in cascade provides a more conservative approach as a starting point. Figure 4 provides a simplified model for analyzing the sensor's response to power application.

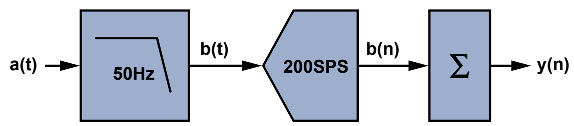

Figure 4. Electrical model for settling time analysis.

After power application, the accelerometer sensor's output, $a(t)$, exhibits a step response. Since the sensor runs off of a single supply, its output will likely start at zero and quickly transition to a level that establishes its orientation. For simplicity, assume that a zero output corresponds to the minimum acceleration level available. In this case, we use $-2\ g$, in order to provide some margin over the specified minimum of $-1.7\ g$. Also, the maximum incline range is +30°, which is equivalent to $+0.5\ g$. Combining these two intervals, the maximum transition that the accelerometer signal will make at startup is $+2.5\ g$. The step response of the single-pole, low-pass filter, $b(t)$, is captured in the following formula:

$$a(t) = 0, t < 0$$

$$a(t) = 2.5g, t \geq 0$$

$$b(t) = 2.5 \times \left(1 - e^{-100\pi t}\right)$$

A model that includes the digital filter requires a discrete version of $b(t)$, along with a summation model to simulate the filter.

$$b(n) = b(t), t = \frac{n}{f_S} = \frac{n}{200}$$

$$b(n) = 2.5 \times \left(1 - e^{-\frac{\pi}{2}}\right)$$

$$y(n) = \frac{1}{N}\sum_{n=1}^{N} b(n) = \frac{2.5}{N}\sum_{n=1}^{N}\left(1 - e^{-\frac{\pi}{2}}\right)$$

The settling time is the time required to settle to its final value within a specified accuracy, A_E. Figure 5 shows two transient response curves and indicates the settling time for each to an accuracy of $0.1\ g$.

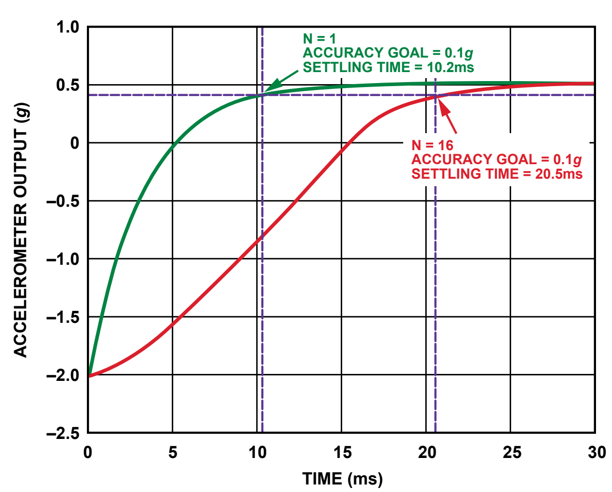

Figure 5. Power-on transient response.

For this example, the error budget allows 0.2° of settling accuracy. The sine formula provides a simple method for translating this goal into an acceleration metric.

$$a_{g\,\max} = \sin 0.2° \approx 3.5\ \text{m}g$$
$$a_{g\,\min} = \sin 30° - \sin 29.8° \approx 3.0\ \text{m}g$$

Modeling this formula is very simple with tools like Excel or MATLAB. When using Excel, the output reaches a level within 3 mg of 0.5 g on the 18th sample when N = 16—and on the 65th sample when N = 64. Dividing each of these numbers by the sample rate (200 SPS) provides settling time estimates for these settings of 21 ms for N = 1, 90 ms for N = 16, and 325 ms for N = 64. Assume (if reasonable) that the errors associated with thermal settling are negligible. Since the device being considered provides a temperature calibrated response, this is probably an acceptable assumption. Validating this assumption offers a good opportunity to verify the accuracy as part of the final characterization process.

The data-acquisition time, T_3, for this type of system doesn't need to be longer than one sample cycle, since all of the necessary correction and filtering is handled inside the device. Here, the acquisition time will only contribute 5 ms to the overall measurement time.

4. Relate Power Dissipation to Cycle Time

The final part of this analysis relates the average power dissipation and the cycle time, which is, in effect, equal to the amount of time between individual measurement events. Table 2 summarizes key power cycling factors, either specified in the sensor's data sheet or produced through this simple analysis process, including numbers for both full start-up (power cycling) and sleep-mode recovery (sleep cycling).

Table 2. Summary of Critical Power Cycling Parameters

	Power Cycling	**Sleep Cycling**
P_{ON}	46.2 mW	
P_{OFF}	3.3 μW	1.15 mW
T_M, N = 1	190 + 21 + 5 = 216 ms	2.5 + 21 + 5 = 28.5 ms
T_M, N = 16	190 + 90 + 5 = 285 ms	2.5 + 90 + 5 = 97.5 ms
T_M, N = 64	190 + 325 + 5 = 520 ms	2.5 + 325 + 5 = 332.5 ms

The following calculation provides a quick example for using these parameters to analyze and compare power cycling and sleep cycling for a system that requires a measurement rate of 1 SPS.

Power cycling:

$$D = \frac{T_{ON}}{T_{ON} + T_{OFF}} = \frac{T_{ON}}{T_C} = \frac{0.216\ \text{s}}{1\ \text{s}} = 0.216$$
$$P_{AVG} = [D \times P_{ON}] + [(1 - D) \times P_{OFF}]$$
$$P_{AVG} = [0.216 \times 0.0462] + [0.784 \times 0.0000033] = 0.00998\ \text{W}$$
$$P_{AVG} \approx 10\ \text{mW}$$

Sleep cycling:

$$D = \frac{T_{ON}}{T_{ON} + T_{OFF}} = \frac{T_{ON}}{T_C} = \frac{0.0285\ \text{s}}{1\ \text{s}} = 0.0285$$
$$P_{AVG} = [D \times P_{ON}] + [(1 - D) \times P_{OFF}]$$
$$P_{AVG} = [0.0285 \times 0.0462] + [0.9715 \times 0.00115] = 0.00243\ \text{W}$$
$$P_{AVG} \approx 2.4\ \text{mW}$$

Here sleep cycling is advantageous. However, if the cycle time was increased to one sample per minute (T_C = 60 s), the average power dissipation would be 0.2 mW for the power cycling approach and 1.2 mW for the sleep cycling approach. A useful graphical relationship between cycle time and average power dissipation is shown in Figure 6.

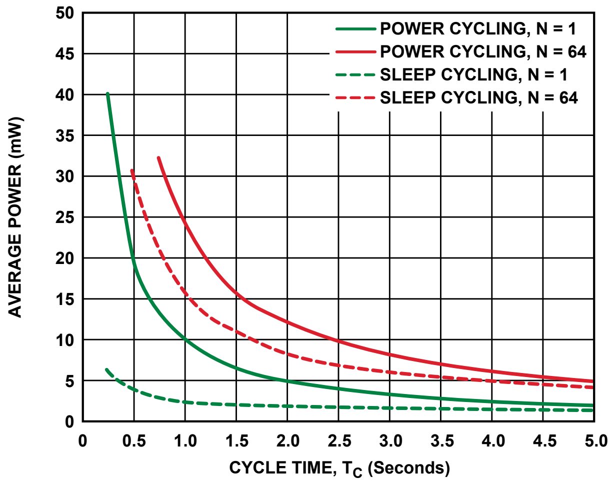

Figure 6. Cycle time vs. average power dissipation.

The *sleep* mode keeps all of the initialization values while shutting down the rest of the system. Although maintaining these settings requires some power, recovery times are faster than full start-up times. The ADIS16209 tilt sensor provides a programmable sleep time and automatic wake-up. This type of solution fits well with a master processor that can also wake up on a data-ready signal, take the data it needs, and command the sensor to go back to sleep for another fixed period. Another example of a MEMS product that uses *sleep* mode is the ADIS16223 vibration sensor, which collects and stores vibration data, automatically goes back into sleep mode, and then starts a countdown to another measurement event. This type of sensor works well for systems that require periodic monitoring, without the need to assign processor resources to manage the sleep and data collection modes.

This simple analysis provides some useful insights. In particular, there are some cases where, despite the power required in sleep mode, sleep-mode management can offer energy savings. In the above example, sleep mode offered a 4:1 improvement for systems that need tilt measurements at a rate of 1 SPS. Here, the sleep mode provides power saving for measurement cycle times up to 6 s. For systems that have longer measurement cycle times, the lower overhead associated with managing a shutdown feature enables lower average power levels.

Conclusion

Whether for economic or environmental reasons, the desire to reduce power consumption seems to be nearly universal. Reducing power consumption can reduce the size and cost of power sources, such as power converters, batteries, and solar cells. Other potential benefits include relaxed thermal and mechanical design requirements, lower EMI emissions, and more favorable environmental impact ratings.

The concepts and analysis techniques presented in this article provide a good starting point for engineers who value highly integrated sensor products but are also under pressure to reduce power consumption where possible. More importantly, the thought process associated with identifying and analyzing behaviors that can impact overall power goals will be even more important, as each system design offers new opportunities and risks. After completing the initial analysis, perhaps the Russian proverb, "Доверяй, но проверяй`" ("Trust, but verify!"), best summarizes how to assure success in the final implementation. Keep track of key assumptions, such as the settling accuracy (3 m*g*) and whether thermal settling will play a role. When appropriate hardware is available, test these solutions in conditions that match their intended use as closely as possible. In the end, testing these assumptions will add confidence and refine new assumptions for future analysis of power management techniques.

Appendix

The ADIS16209 *i*Sensor® dual-axis inclinometer (Figure A) provides a digital output proportional to the rotation in one plane parallel to the Earth's gravity (vertical mode) over a ±180° range, or two planes tangential to the Earth's gravity (horizontal mode) over a ±90° range. The on-chip ADC digitizes the output of the *i*MEMS® accelerometers, the internal temperature sensor, the power supply, and an auxiliary analog input, and provides the data via an SPI-compatible interface. Sensitivity, sample rate, bandwidth, and alarm thresholds are all digitally programmable. Functionally complete, the device also includes an auxiliary 12-bit DAC, precision 2.5-V reference, digital self-test function, and programmable power management. Operating with a single 3.0-V to 3.6-V supply, the ADIS16209 consumes 36 mA in fast mode, 11 mA in normal mode, and 140 μA in sleep mode. Available in a 16-terminal LGA package, it is specified from –40°C to +125°C.

The ADIS16223 *i*Sensor digital vibration sensor (Figure B) combines a ±70-*g* single-axis *i*MEMS accelerometer with a flexible, low-power signal processor. The 22-kHz sensor bandwidth and 72.9-kSPS sample rate are well-suited to machine-health applications; an averaging/decimating filter optimizes operation for lower bandwidth applications. The device can capture and store 1k samples from each of three axes using automatic, manual, or event-capture data collection modes. It also measures temperature and supply voltage, captures peaks, and provides a condition-based alarm function. Operating on a single 3.15-V to 3.6-V supply, the ADIS16223 consumes 38 mA in *capture* mode and 230 μA in *sleep* mode. Available in a 16-terminal LGA package, it is specified from –40°C to +125°C.

References

1. ADIS16209 Data Sheet, www.analog.com/ADIS16209.
2. ADIS16223 Data Sheet, www.analog.com/ADIS16223.

Author

Mark Looney [mark.looney@analog.com] is an *i*Sensor application engineer at Analog Devices in Greensboro, NC. Since joining ADI in 1998, he has accumulated experience in sensor signal processing, high-speed analog-to-digital converters, and dc-to-dc power conversion. He earned BS (1994) and MS (1995) degrees in electrical engineering from the University of Nevada, Reno, and has published several articles. Prior to joining ADI, he helped start IMATS, a vehicle electronics and traffic-solutions company, and worked as a design engineer for the Interpoint Corporation.

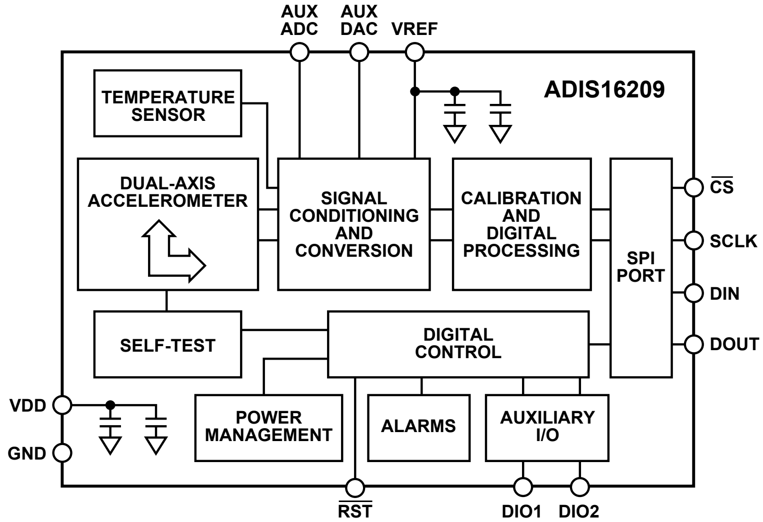

Figure A. ADIS16209 block diagram.

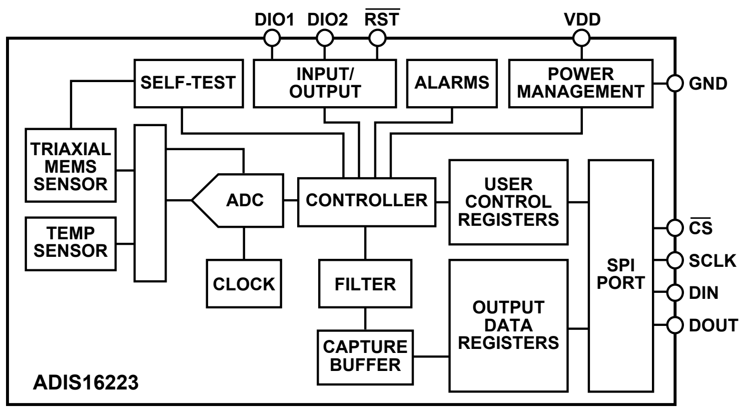

Figure B. ADIS16223 block diagram.